AIP | Applied Physics Letters

Terahertz GaAs/AlAs quantum-cascade lasers

L. Schrottke, X. Lü, G. Rozas, K. Biermann, and H. T. Grahn

Citation: Applied Physics Letters **108**, 102102 (2016); doi: 10.1063/1.4943657
View online: http://dx.doi.org/10.1063/1.4943657
View Table of Contents: http://scitation.aip.org/content/aip/journal/apl/108/10?ver=pdfcov
Published by the AIP Publishing

Terahertz GaAs/AlAs quantum-cascade lasers

L. Schrottke,[a] X. Lü, G. Rozas, K. Biermann, and H. T. Grahn
Paul-Drude-Institut für Festkörperelektronik, Hausvogteiplatz 5–7, 10117 Berlin, Germany

(Received 10 December 2015; accepted 29 February 2016; published online 8 March 2016)

We have realized GaAs/AlAs quantum-cascade lasers operating at 4.75 THz exhibiting more than three times higher wall plug efficiencies than GaAs/$Al_{0.25}Ga_{0.75}As$ lasers with an almost identical design. At the same time, the threshold current density at 10 K is reduced from about 350 A/cm^2 for the GaAs/$Al_{0.25}Ga_{0.75}As$ laser to about 120 A/cm^2 for the GaAs/AlAs laser. Substituting AlAs for $Al_{0.25}Ga_{0.75}As$ barriers leads to a larger energy separation between the subbands reducing the probability for leakage currents through parasitic states and for reabsorption of the laser light. The higher barriers allow for a shift of the quasi-continuum of states to much higher energies. The use of a binary barrier material may also reduce detrimental effects due to the expected composition fluctuations in ternary alloys. © *2016 AIP Publishing LLC*. [http://dx.doi.org/10.1063/1.4943657]

The high-quality growth of complex planar heterostructures with more than one thousand layers has led to the development and application of quantum-cascade lasers (QCLs).[1] While mid-infrared QCLs are often based on the (In,Ga)As/(In,Al)As materials system, QCLs for the terahertz (THz) spectral region[2] utilize mainly GaAs/(Al,Ga)As heterostructures. However, mid-infrared QCLs have also been reported for the GaAs/(Al,Ga)As[3,4] and the GaAs/AlAs system.[5] A particular challenge for the design of GaAs/(Al,Ga)As QCLs is the indirect character of the band offset in the heterostructures for larger Al content.

During the last decade, THz QCLs have been used as radiation sources for modulation spectroscopy,[6] for local oscillators in heterodyne receivers for astronomy,[7–9] and for sophisticated THz imaging techniques.[10] For many of these applications, the continuous-wave (cw) mode is required in order to achieve frequency-stabilized operation. At the same time, cryogenic-liquid-free coolers are preferred. In particular, QCLs used in airborne heterodyne receivers such as the German REceiver for Astronomy at Terahertz (GREAT) frequencies on board of the Stratospheric Observatory For Infrared Astronomy (SOFIA) have to be operated in a mechanical cooler. Recently, 4.75 THz QCLs fulfilling specifications for the use in airborne instruments have been developed.[11,12] The QCL realized recently by our group for GREAT[12] with a target frequency of 4.7448 THz allows for an optical power of 1.2 mW requiring about 4 W of electrical power at 10 K, which corresponds to a wall plug efficiency of 3×10^{-4}. While this laser is based on a single-plasmon waveguide in order to obtain an almost Gaussian beam profile using a TPX lens, an alternative approach comprises the use of metal-metal waveguides with third-order distributed-feedback structures.[11] In Ref. 11, the QCL was reported to provide an optical power of about 0.25 mW at 10 K with an electrical power of about 0.7 W, i.e., a wall plug efficiency of 3.6×10^{-4}. For the use of less demanding cooling systems, an increase in the wall plug efficiency is highly desirable.

The majority of THz QCLs are based on the GaAs/$Al_xGa_{1-x}As$ heterostructures with $0.1 \leq x \leq 0.25$.[13–15] Lower Al content allows for sufficient coupling through thicker injection barriers so that the layer thicknesses can be better controlled during growth. Furthermore, the subband structure is more robust against thickness fluctuations, which facilitates the design. Only a few attempts have been made to use other material systems such as (In,Ga)As/ (In,Al)As and (In,Ga)As/Ga(As,Sb).[16,17] More than 10 years ago, Ulrich *et al.*[18] showed that AlAs barriers allow for a higher electroluminescence efficiency, which was ascribed to a reduction of the alloy scattering in the barriers. Recently, THz QCLs have been presented introducing a tall AlAs barrier in order to reduce parasitic leakage currents.[19] This structure showed an improved temperature performance compared to a sample without the tall barrier grown in the same system, while a design using only AlAs barriers was reported to fail to lase. As a reason, the authors discussed either negative differential conductance (NDC) at low voltages or excessive interface roughness scattering.

In this letter, we demonstrate that replacing the ternary $Al_xGa_{1-x}As$ barriers by binary AlAs layers can lead to more than three times larger wall plug efficiencies. In order to directly compare the operating parameters of those lasers, we adjusted the design B2 of Ref. 9, which is used in GREAT, as little as possible. The barrier thicknesses $L_{B,1}$ of the design with $Al_{0.25}Ga_{0.75}As$ barriers were scaled down to obtain the values $L_{B,2}$ for the GaAs/AlAs structure according to the barrier heights, i.e., the conduction band offsets ΔE_C, using the scaling relation,[15]

$$\frac{L_{B,1}}{L_{B,2}} = \sqrt{\frac{\Delta E_{C,2}}{\Delta E_{C,1}}}.$$

The barrier thicknesses were rounded to integer values of monolayers (MLs) with a minimum thickness of 2 MLs. The quantum well thicknesses have been adjusted so that the subband structures of the two designs are very similar. The injection barriers are thinner than determined by the scaling relation in order to compensate for the influence of interface grading[20,21] on the coupling strength between wave functions close to the GaAs conduction band edge. For the band offsets, we used $\Delta E_{C,1} = 232$ meV and $\Delta E_{C,2} = 982$ meV.

[a]Electronic mail: lutz@pdi-berlin.de

For a refined scaling of the barrier thicknesses, more sophisticated methods such as *inverse-quantum-engineering*[22] may be applied.

Figure 1 shows the potential profile and the squared moduli of the wave functions for both designs. The structure with $Al_{0.25}Ga_{0.75}As$ barriers shown in Fig. 1(a) exhibits a somewhat larger miniband width due to the stronger coupling through the lower barriers than the structure with AlAs barriers shown in Fig. 1(b). Similarly, the coupling through the injection barrier is stronger. In order to compensate the weaker coupling in the structure with AlAs barriers, the doping for this design was increased. Furthermore, the state R, which leads to reabsorption by electronic transitions from the upper laser level, is shifted to much higher energies. Similarly, the state P, which may be responsible for leakage from the miniband directly to the lower laser level, is shifted and completely decoupled from the other wave functions. All relevant states in the GaAs/AlAs structure are well below the *X* minimum of the AlAs band structure schematically indicated by the dashed line. Therefore, Γ-*X*-Γ transfer is expected to be negligible.

Figures 2(a) and 2(b) show the calculated gain maps for the designs employing $Al_{0.25}Ga_{0.75}As$ and AlAs barriers, respectively, using a self-consistent rate equation model.[24] In both designs, the gain maximum is close to the target frequency of 4.7448 THz with the onset of the gain at somewhat lower field strengths for the GaAs/AlAs structure. Both structures show a similar red shift of the gain maximum with increasing electrical field strength. The calculated current density-electric field strength characteristics, as shown in Figs. 2(c) and 2(d), exhibit larger current densities for the design with the $Al_{0.25}Ga_{0.75}As$ barriers with a similar shape of the curve, despite the different doping density. Note that the applied model does not completely reflect the coupling properties since coherent processes[25–27] are not included so that the accuracy of the absolute values must not be overestimated. Furthermore, the effect of the doping density is reduced by the formation of an intra-period dipole-like space charge.

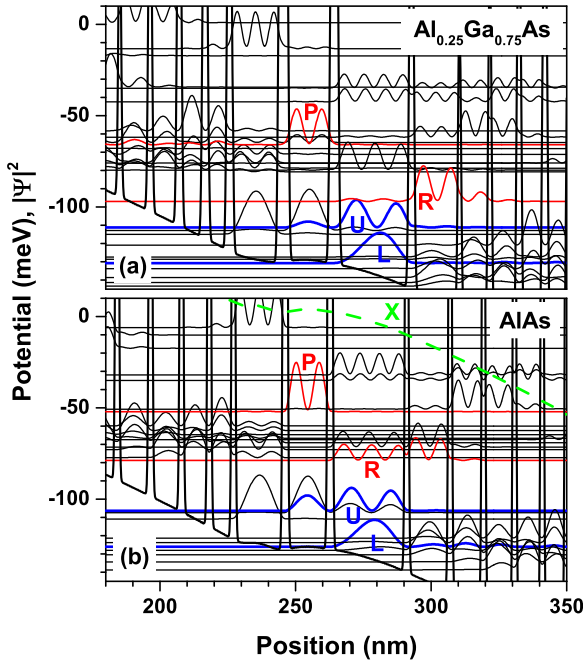

FIG. 1. Potential profile and subband structure (moduli squared of the envelope functions) at an applied field strength of 5 kV/cm for the QCLs with (a) $Al_{0.25}Ga_{0.75}As$ barriers and (b) AlAs barriers. The layer sequences starting from the injection barrier are (a) **3.3**, 25.9, **1.9**, 16.3, **0.9**, 10.1, **1.3**, 9.2, **1.8**, 7.6, **2.1**, 6.9, **2.1**, 16.9, **3.8**, 15.2 (cf. design B2 in Ref. 9) and (b) **1.12**, 27.4, **0.56**, 15.4, **0.56**, 11.8, **0.56**, 10.8, **0.56**, 9.7, **0.56**, 8.4, **0.56**, 18.2, **1.12**, 15.5 with the layer thicknesses in nm. Bold characters denote the barriers, while the underlined numbers indicate the doped layers. The nominal doping densities for (a) and (b) are 8×10^{16} and 2×10^{17} cm^{-3}, respectively. The simulations include interface grading with a grading parameter of 0.28 nm (1 ML) as defined in Ref. 20. The upper and lower laser levels are marked as U and L, respectively. R denotes states leading to reabsorption of the laser light and P parasitic states, which may open leakage channels. The dashed line in (b) shows the energy of 130 meV above the GaAs band edge corresponding to the *X* minimum of the AlAs band structure.[23]

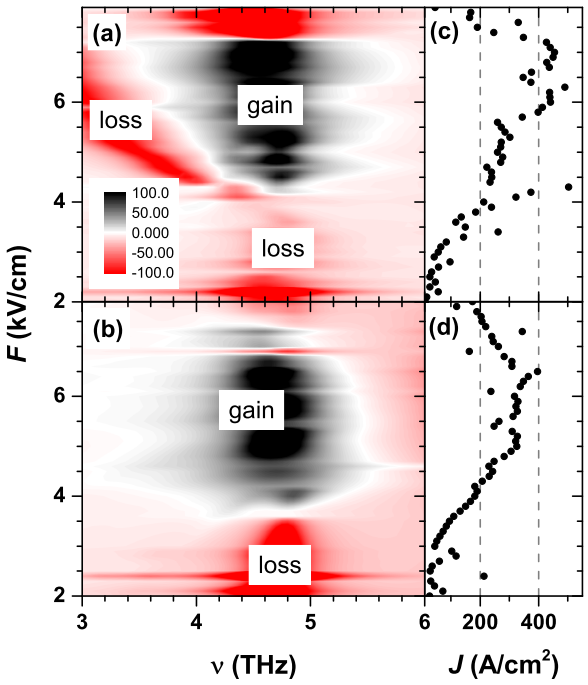

FIG. 2. Calculated gain maps as a function of frequency ν and electric field strength F for the structure with (a) $Al_{0.25}Ga_{0.75}As$ barriers and (b) AlAs barriers for the parameters given in Fig. 1. Calculated current density-applied field strength (J-F) characteristics for the respective structures are shown in panels (c) and (d).

Two GaAs/AlAs QCLs with a target frequency of 4.7448 THz were grown using molecular beam epitaxy on semi-insulating GaAs wafers for processing into single-plasmon waveguides and Fabry-Pérot ridge lasers. As the reference laser for the comparison with QCLs employing $Al_{0.25}Ga_{0.75}As$ barriers, we used the laser selected for use in GREAT out of a larger series of lasers.[28] This QCL ranks among the best with respect to frequency *and* threshold current density. Both lasers consist of 88 periods with a total thickness of about 11 ($Al_{0.25}Ga_{0.75}As$) and 10.8 μm (AlAs). The growth of the very thin AlAs barriers with 2–4 ML thickness is rather challenging. The straightforward way to increase the Al shutter opening time for such a thin AlAs layer would be to substantially decrease the AlAs growth rate. However, this would lead to very different V/III flux ratios during the growth of the AlAs and GaAs layers, since the As_4 flux cannot be adjusted individually for every single layer, but is kept constant throughout

the growth of the whole cascade structure. Our trade-off approach comprises nominal growth rates of 0.11 nm/s and 0.17 nm/s for AlAs and GaAs, respectively, leading to a minimum Al shutter opening time of 5 s for the thinnest barrier and an overall growth time of about 18 h for the cascades as compared to about 7 s and 17 h, respectively, for QCLs with $Al_{0.25}Ga_{0.75}As$ barriers. The average growth rates were 0.174 and 0.164 nm/s for the GaAs/$Al_{0.25}Ga_{0.75}As$ and GaAs/AlAs samples, respectively, similar to the growth conditions for other THz QCLs grown in the same machine. Using a closed-loop rate control system based on optical reflection measurements, fluctuations in growth rates can be kept below 1%. Furthermore, x-ray diffraction data as shown in Fig. 3 exhibit a deviation of the period length of about 2% of the nominal values. During growth, the substrate was rotated at a speed of 12.04 rpm, which corresponds to 150 rotations per period. Typically, we observe a parabolic decrease of the growth rates from the center to the edge of the 2-in. substrate. At a distance of 20 mm, the GaAs (AlAs) growth rate is about 1.5% (3.0%) smaller than at the center.

The samples were processed by photolithography and standard wet chemical etching for the (Al,Ga)As materials system using an identical procedure for all lasers. The etching solution is H_2SO_4:H_2O_2:H_2O (1:1:8). The role of oxidation of the AlAs for device stability is subject to a long-term observation. However, we do not expect severe problems since GaAs/AlAs superlattices have been extensively investigated for decades even for rather sophisticated effects.[29] Furthermore, a study of the growth conditions with respect to interface roughness or background doping level[30] on the operating properties may improve the device characteristics.

The QCLs were measured in a He-flow cryostat with a polyethylene window. The output power was detected using a commercial, calibrated pyroelectric power meter,[31] while the laser emission spectra were recorded using a Fourier transform infrared spectrometer. In order to rule out possible modifications of the collection efficiency, the data for the GaAs/AlAs QCL were measured immediately after the GaAs/$Al_{0.25}Ga_{0.75}As$ QCL using the same setup, and the lasers were operated under identical conditions. Furthermore, different values for the thermal conductance of the samples may have an effect on the operating properties under cw operation so that the experiments focused on pulsed operation. Figures 4(a) and 4(b) show the experimental light output-current density-voltage (*L-J-V*) characteristics of the two QCLs. Both lasers exhibit similar maximum optical output power of about 8 mW at 10 K. However, the corresponding current densities for the QCL with the AlAs barriers are smaller by a factor of approximately 2 over the whole range. The threshold current density is about 120 A/cm^2 for the GaAs/AlAs QCL, while the value is about 340 A/cm^2 for the GaAs/$Al_{0.25}Ga_{0.75}As$ QCL. At the same time, the corresponding measured as well as simulated voltage values (cf. Fig. 2) are also smaller so that the (pulse mode) wall plug efficiency for the laser with the AlAs barriers reaches about 1.2×10^{-3}, while the value is 3.2×10^{-4} for the QCL with the $Al_{0.25}Ga_{0.75}As$ barriers. Figure 5(a) displays measured spectra of the GaAs/AlAs QCL for several operating conditions, which shows that the target frequency of 4.7448 THz is well included in the mode spectra of this QCL.

The significantly higher wall plug efficiency of the QCL with the AlAs barriers compared to the GaAs/$Al_{0.25}Ga_{0.75}As$ QCL is a clear indication of substantially reduced leakage currents. The reduced pumping energy can in part be explained by the design improvements discussed above such as the shift of levels R (reabsorption) and P (leakage). In addition, leakage into quasi-continuum states, which are shifted to much higher energies, may be reduced. The somewhat weaker coupling through the AlAs barriers may also affect the coherent transport. In addition, the improvements may also be explained by reduced composition fluctuations in the barriers. Due to interface grading, the Al content in the rather thin AlAs barriers does not reach 100%. Assuming an interface parameter of 1 ML, the injection barriers consisting of nominally 4 MLs have

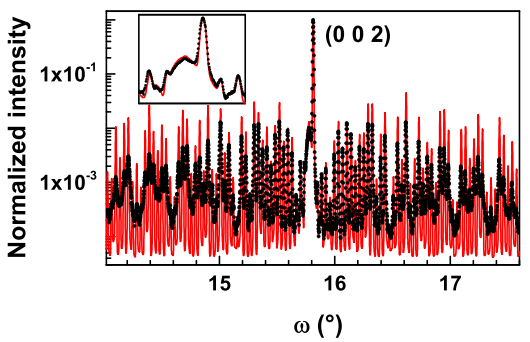

FIG. 3. X-ray diffraction $\omega(2\theta)$ scan around the (002) reflection for the AlAs sample with the lower doping density (symbols). The line represents a simulation of the QCL structure with layer thicknesses of 1.022 times larger than the nominal values. The inset shows the data close to the (002) reflection on an enlarged scale.

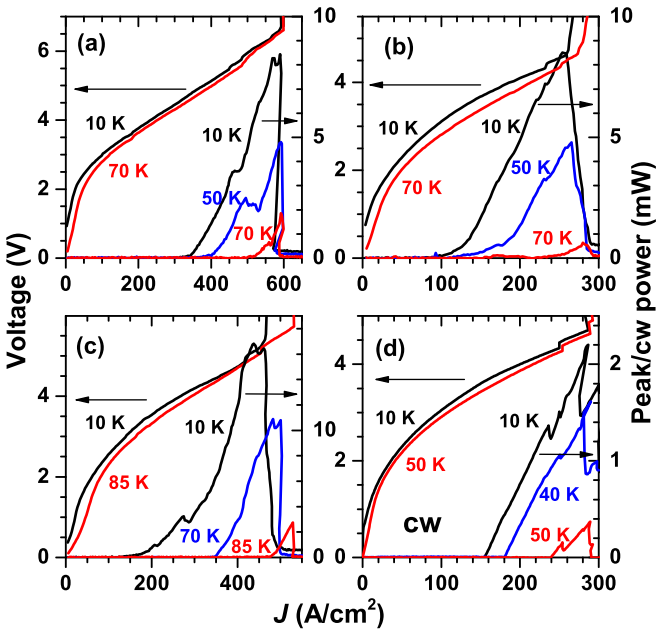

FIG. 4. *L-J-V* characteristics for pulsed operation for the QCLs (a) with $Al_{0.25}Ga_{0.75}As$ barriers, a doping density of 8×10^{16} cm^{-3}, and laser ridge dimensions of 0.2×3.38 mm^2, (b) with AlAs barriers, a doping density of 2×10^{17} cm^{-3}, and ridge dimensions of 0.2×3.0 mm^2, as well as (c) with AlAs barriers, a doping density of 3×10^{17} cm^{-3} and laser ridge dimensions of 0.2×3.0 mm^2 at several operating temperatures as indicated. The pulse duration was 500 ns at a repetition rate of 5 kHz. (d) *L-J-V* characteristics for cw operation for the GaAs/AlAs QCL with a doping density of 2×10^{17} cm^{-3} and laser ridge dimensions of 0.12×1.11 mm^2 at several operating temperatures as indicated.

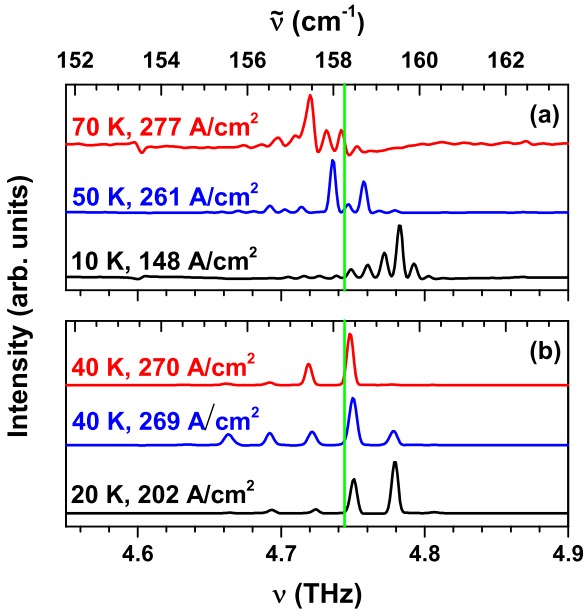

FIG. 5. Lasing spectra of the QCL with AlAs barriers and a doping density of 2×10^{17} cm^{-3} for (a) pulsed operation (0.2×3.0 mm^2 ridge) and (b) cw operation (0.12×1.11 mm^2 ridge) for several operating temperatures and current densities. The vertical solid line indicates the target frequency of 4.7448 THz.

a maximum Al content of about 80% in the center of the layers. The thinner barriers in the quasi-miniband region consisting of 2 MLs have a maximum Al content of about 50%, while the thicker injection barriers of the GaAs/$Al_{0.25}Ga_{0.75}As$ QCL have a maximum Al content of 25%. According to Kim *al.*,[32] composition fluctuations of the barrier material may lead to additional leaky states and open *low-potential channels*. We assume that these additional states occur at significantly higher energies for the AlAs injection barriers than for the AlAs barriers in the quasi-miniband region and even more pronounced than for the ternary $Al_{0.25}Ga_{0.75}As$ barriers. Therefore, leakage currents bypassing the laser states are possibly reduced by using AlAs for the injection barriers.

In addition, the role of interface scattering needs to be considered in more detail. Although the higher barriers lead to larger scattering due to interface roughness,[19,33] the wave functions of the laser levels for the applied hybrid design with a vertical lasing transition show an almost negligible amplitude at the interfaces so that interface scattering is very small. Furthermore, the constituent wave functions of the quasi-miniband are indeed exposed to increased interface scattering, and pure miniband transport is reduced. However, the above mentioned composition fluctuations may open additional transport channels, since we expect the additional states to occur at lower energies than for the injection barriers.

To show the reliability of the rather thin AlAs barriers, a second structure for the same target frequency with a nominally identical layer sequence but an increased doping density from 2×10^{17} to 3×10^{17} cm^{-3} was investigated. The *L-J-V* characteristics as shown in Fig. 4(c) exhibit current densities at threshold (200 A/cm^2) as well as at the maximum output power (450 A/cm^2), which are about 1.5 times larger than for the sample with a doping density of 2×10^{17} cm^{-3}. At the same time, the maximum output power of 16 mW is almost doubled, i.e., the (pulse mode) wall plug efficiency is again about 1.2×10^{-3}. Furthermore, the maximum operating temperature is increased from about 70 to about 85 K.

As shown by the *L-J-V* characteristics in Fig. 4(d) for cw operation of a GaAs/AlAs laser (0.12×1.11 mm^2 ridges) with the lower doping density, the wall plug efficiency reaches again about 1.2×10^{-3}. The mode spectra including the target frequency are shown in Fig. 5(b). While the temperature-dependent optical output power[31] is similar to the values obtained from the laser used in GREAT, the electrical pumping power is reduced. Therefore, also the required cooling power is reduced, and/or a lower operating temperature can be achieved using the Stirling cooler. Furthermore, a similar QCL with a preliminary design using the AlAs barriers operating at about 3.4 THz in pulse mode exhibits also a very small threshold current density. However, this laser suffers from an NDC at lower field strengths (cf. Ref. 19). In our preliminary design with a rather low doping density (5×10^{16} cm^{-3}), the interplay between the dipole-like space charge and the simultaneous coupling of the laser levels to the injector and the extraction miniband has still to be optimized in order to shift the NDC to higher field strengths. Therefore, the maximum optical power of this laser is still rather small.

In summary, QCLs based on the GaAs/AlAs heterostructures exhibit superior operating parameters over lasers with $Al_{0.25}Ga_{0.75}As$ barriers at least for the employed hybrid design with a vertical optical transition. In particular, the (pulse mode as well as cw) wall plug efficiency can be significantly increased. We believe that the design as well as the balance between barrier thicknesses and doping density for the GaAs/AlAs QCLs can be further optimized so that improvements with respect to other operating parameters are also expected. In addition, the possibility of employing AlAs alternatively to $Al_xGa_{1-x}As$ barriers for THz QCLs enhances the flexibility in the design of these devices.

The authors would like to thank M. Höricke, W. Anders, and A. Riedel for sample preparation, B. Röben and M. Hempel for helpful discussions as well as U. Jahn for a careful reading of the manuscript.

[1]J. Faist, F. Capasso, D. L. Sivco, C. Sirtori, A. L. Hutchinson, and A. Y. Cho, Science **264**, 553 (1994).
[2]R. Köhler, A. Tredicucci, F. Beltram, H. E. Beere, E. H. Linfield, A. G. Davies, D. A. Ritchie, R. C. Iotti, and F. Rossi, Nature **417**, 156 (2002).
[3]C. Sirtori, P. Kruck, S. Barbieri, P. Collot, J. Nagle, M. Beck, J. Faist, and U. Oesterle, Appl. Phys. Lett. **73**, 3486 (1998).
[4]H. Page, C. Becker, A. Robertson, G. Glastre, V. Ortiz, and C. Sirtori, Appl. Phys. Lett. **78**, 3529 (2001).
[5]C. Becker, C. Sirtori, H. Page, G. Glastre, V. Ortiz, X. Marcadet, M. Stellmacher, and J. Nagle, Appl. Phys. Lett. **77**, 463 (2000).
[6]R. Eichholz, H. Richter, M. Wienold, L. Schrottke, R. Hey, H. T. Grahn, and H.-W. Hübers, Opt. Express **21**, 32199 (2013).
[7]J. R. Gao, J. N. Hovenier, Z. Q. Yang, J. J. A. Baselmans, A. Baryshev, M. Hajenius, T. M. Klapwijk, A. J. L. Adam, T. O. Klaassen, B. S. Williams, S. Kumar, Q. Hu, and J. L. Reno, Appl. Phys. Lett. **86**, 244104 (2005).
[8]H.-W. Hübers, S. G. Pavlov, A. D. Semenov, R. Köhler, L. Mahler, A. Tredicucci, H. E. Beere, D. A. Ritchie, and E. H. Linfield, Opt. Express **13**, 5890 (2005).
[9]L. Schrottke, M. Wienold, R. Sharma, X. Lü, K. Biermann, R. Hey, A. Tahraoui, H. Richter, H.-W. Hübers, and H. T. Grahn, Semicond. Sci. Technol. **28**, 035011 (2013).

[10]P. Dean, A. Valavanis, J. Keeley, K. Bertling, Y. L. Lim, R. Alhathlool, A. D. Burnett, L. H. Li, S. P. Khanna, D. Indjin, T. Taimre, A. D. Rakić, E. H. Linfield, and A. G. Davies, J. Phys. D: Appl. Phys. **47**, 374008 (2014) and references therein.
[11]J. L. Kloosterman, D. J. Hayton, Y. Ren, T. Y. Kao, J. N. Hovenier, J. R. Gao, T. M. Klapwijk, Q. Hu, C. K. Walker, and J. L. Reno, Appl. Phys. Lett. **102**, 011123 (2013).
[12]H. Richter, M. Wienold, L. Schrottke, K. Biermann, H. T. Grahn, and H.-W. Hübers, IEEE Trans. Terahertz Sci. Technol. **5**, 539 (2015).
[13]B. S. Williams, Nat. Photonics **1**, 517 (2007) and references therein.
[14]C. Walther, M. Fischer, G. Scalari, R. Terazzi, N. Hoyler, and J. Faist, Appl. Phys. Lett. **91**, 131122 (2007).
[15]M. Wienold, L. Schrottke, M. Giehler, R. Hey, W. Anders, and H. T. Grahn, Appl. Phys. Lett. **97**, 071113 (2010).
[16]M. Fischer, G. Scalari, K. Celebi, M. Amanti, Ch. Walther, M. Beck, and J. Faist, Appl. Phys. Lett. **97**, 221114 (2010).
[17]C. Deutsch, M. Krall, M. Brandstetter, H. Detz, A. M. Andrews, P. Klang, W. Schrenk, G. Strasser, and K. Unterrainer, Appl. Phys. Lett. **101**, 211117 (2012).
[18]J. Ulrich, G. Strasser, and K. Unterrainer, Physica E **13**, 900 (2002).
[19]C. W. I. Chan, Q. Hu, and J. L. Reno, Appl. Phys. Lett. **103**, 151117 (2013).
[20]E. Luna, F. Ishikawa, P. D. Batista, and A. Trampert, Appl. Phys. Lett. **92**, 141913 (2008).
[21]X. Lü, L. Schrottke, E. Luna, and H. T. Grahn, Appl. Phys. Lett. **104**, 232106 (2014).
[22]I. Waldmueller, M. C. Wanke, M. Lerttamrab, D. G. Allen, and W. W. Chow, IEEE J. Quantum Electron. **46**, 1414 (2010).
[23]I. Vurgaftman, J. R. Meyer, and L. R. Ram-Mohan, J. Appl. Phys. **89**, 5815 (2001).
[24]L. Schrottke, X. Lü, and H. T. Grahn, J. Appl. Phys. **117**, 154309 (2015).
[25]S. Kumar and Q. Hu, Phys. Rev. B **80**, 245316 (2009).
[26]E. Dupont, S. Fathololoumi, and H. C. Liu, Phys. Rev. B **81**, 205311 (2010).
[27]G. Beji, Z. Ikonić, C. A. Evans, D. Indjin, and P. Harrison, J. Appl. Phys. **109**, 013111 (2011).
[28]M. Wienold, B. Röben, X. Lü, G. Rozas, L. Schrottke, K. Biermann, and H. T. Grahn, Appl. Phys. Lett. **107**, 202101 (2015).
[29]Y. Huang, H. Qin, W. Li, S. Lu, J. Dong, H. T. Grahn, and Y. Zhang, Europhys. Lett. **105**, 47005 (2014).
[30]L. H. Li, J. X. Zhu, L. Chen, A. G. Davies, and E. H. Linfield, Opt. Express **23**, 2720 (2015).
[31]Power values are not corrected for window transmission losses or collection efficiency and are a lower bound by a factor of about 2 to the absolute power of the lasers. For cw measurements, the values are corrected by a factor of 3.3 with respect to pulsed measurements in order to take into account a smaller collection efficiency due to different experimental setups.
[32]D. S. Kim, H. S. Ko, Y. S. Lim, Y. M. Kim, J. S. Lee, S. J. Rhee, W. S. Kim, S. C. Hong, Y. H. Yee, J. S. Khim, J. M. Jung, S. Huhr, J. H. Lee, J. S. Chang, B. D. Choe, J. C. Woo, P. H. Song, H. J. Choi, S. H. Jhi, J. Ihm, E. J. Shin, D. Kim, D. H. Woo, K. N. Kang, and J. J. Song, J. Opt. Soc. Am. B **13**, 1210 (1996).
[33]C. Deutsch, H. Detz, T. Zederbauer, A. M. Andrews, P. Klang, T. Kubis, G. Klimeck, M. E. Schuster, W. Schrenk, G. Strasser, and K. Unterrainer, Opt. Express **21**, 7209 (2013).